Prolines are not essential residues in the "barrel-stave" model for ion channels induced by alamethicin analogues

Hervé Duclohier, Gérard Molle, Jean-Yves Dugast, and Gérard Spach
URA 500 CNRS, Faculté des Sciences, Université de Rouen, BP 118, 76134 Mont-Saint-Aignan, France

ABSTRACT In the "barrel-stave" model for voltage-gated alamethicin channels in planar lipid bilayers, proline residues, especially Pro_{14}, are assumed to play a significant role. Taking advantage of a previous synthetic alamethicin analogue in which all eight α-aminoisobutyric acids were replaced by leucines, two new analogues were prepared in order to test the effects of Pro_{14} and Pro_2 substitutions by alanines. The α-helical content of the three analogues in methanol solution remains predominant (between 63 and 80%). Macroscopic conductance experiments show that a high voltage dependence is conserved, although the apparent mean number of monomers forming the channels is significantly reduced when the substitution occurs at position 14. This is confirmed in single-channel experiments which further reveal faster fluctuations for the modified analogues. These results demonstrate that, although prolines, especially Pro_{14}, are favorable residues for alamethicin-like events, they are not absolute prerequisites for the development of highly voltage-dependent multistate conductances.

INTRODUCTION

Ion channels can be modeled by aggregates of amphipathic and helical peptides (1). Alamethicin is certainly still the best characterized voltage-dependent channel forming peptide and there now seems to be a consensus for the "barrel-stave" model to account for its conductance properties in lipid bilayers (2–5). A great emphasis is placed upon a proline residue at position 14 leaving the C-terminus lying flat on the bilayer. The application of an electric field would favor either a coil-helix transition or an alignment of this C-terminal segment with the remainder of the molecule already embedded in the bilayer. Alamethicin molecules could then be buried, able to fully span the bilayer and form multi-state channels through the uptake and release of monomers via the lipid matrix (3).

Since eight out of the twenty residues of alamethicin are the noncoded α-aminoisobutyric acids (Aib), difficult to assemble in solid-phase peptide synthesis, we first prepared an analogue in which all Aibs were substituted by leucines with the additional advantage of getting closer to the natural sequences. This peptide (referred thereafter as diBL) induced conductance properties in planar lipid bilayers (6) similar to those of alamethicin (2) and thus offered the opportunity of testing the role of Pro_{14}, underlined as a critical residue for channel stabilization (7) and voltage dependence (8). In addition, the effect of another proline, in position 2 near the N-terminus and missing in certain natural peptaibols (9), was also studied. As a rule, these prolines were substituted by alanines, and thus the sequences of these three analogues are the following:

—diBL :

2

Ac-Leu-Pro-Leu-Ala-Leu-Ala-Gln-Leu-Val-Leu-Gly-Leu-

14 20

Leu-Pro-Val-Leu-Leu-Glu-Gln-Pheol

—diBLP2A :

Ac-Leu-Ala-Leu-Ala-Leu-Ala-Gln-Leu-Val-Leu-Gly-

Leu-Leu-Pro-Val-Leu-Leu-Glu-Gln-Pheol

—diBLP14A :

Ac-Leu-Pro-Leu-Ala-Leu-Ala-Gln-Leu-Val-Leu-Gly-

Leu-Leu-Ala-Val-Leu-Leu-Glu-Gln-Pheol.

Here, we present the effects of such substitutions on the secondary structure assessed by circular dichroism and on macroscopic and single-channel conductances.

MATERIALS AND METHODS

The solid-phase technique (10) was used to prepare the three analogues. The protocol, summarized elsewhere (11) for amidated peptides, was modified to yield the amino-alcohol at the C-terminus (12). Briefly, t-Boc-Pheol was first esterified with succinic anhydride and then coupled to the benzhydrylamino resin (reticulated by 1% divinylbenzene). The synthesis proceeded stepwise towards the N-terminus using t-Boc protected amino-acids with *N*-Hydroxybenzotriazole and *N-N'*-dicyclohexyl-carbodiimide as co-reagents (glutamine had to be coupled as the activated ester). After each step, a Kaiser test allowed the estimation of the coupling yield. Some coupling steps had to be repeated and acetylation was used to block the remaining free NH_2 groups. Providing a negative Kaiser test, the amine function was deprotected with TFA (trifluoroacetic acid, 30% in CH_2Cl_2), then the resin was neutralized by DIEA (diisopropylethylamine, 10% in CH_2Cl_2) before coupling the following amino acid.

After completion of the synthesis and acetylation of the N-terminus, the peptide was released from the resin by a saponification reaction instead of the usual HF treatment. The lyophilized raw products were purified by HPLC (LKB system) through repeated steps on an inverse phase column (C-8, 5 μm, 4.6 × 250 mm; from Société Française Chromato Colonne) under MeOH/H_2O or EtOH/H_2O gradients. Ethanol had to be used in the later steps of purification since some (albeit lim-

0006-3495/92/09/868/06 $2.00

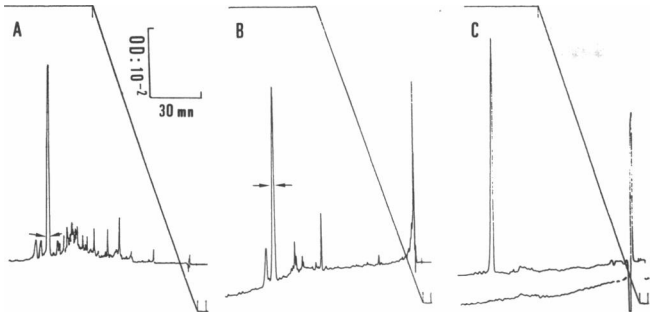

FIGURE 1 HPLC chromatograms of peptide diBLP14A through successive steps. (*A*) Raw product; (*B*) the eluate between arrows in *A* had been reinjected; (*C*) final purification (reinjection of the main peak in *B* collected between arrows); below is shown the blank. Same mobile phase throughout: gradient beginning with MeOH (in *A*) or EtOH (in *B* and *C*)/H_2O/TFA (trifluoroacetic acid) [60/40/0.025] and ending with MeOH or EtOH/H_2O/TFA [90/10/0.025]. Absorption monitored at 206 nm in *A* and 226 nm in *B* and *C*.

ited) interconversion of the main peak towards a secondary one did occur, presumably through methylation of Glu_{18}. Final purity was greater than 98%. Chromatograms are presented in Fig. 1 for the case of diBLP14A, this peptide being by far the most interesting in this work.

Fast Atomic Bombardment (FAB) positive ion mass spectrometry allowed an unambiguous characterization (see reference 13 for review) of the purified peptides. Since Pro residues enhance the fragmentation rate, the interpretation of the diBLP14A spectrum (shown in Fig. 2) was less straightforward than the spectra of the other two analogues. Nevertheless, examination of the fragments masses both from the C-terminus (B-type ions) and from the N-terminus (Y"-type ions), as well as the protonated molecular ion, confirms the sequence generated during the chemical synthesis. The additional unit mass accounts for the statistical abundance of the C^{13} isotope. Table 1 shows experimental molecular masses very close to the expected ones for the three analogues.

Circular dichroism spectra of the peptides in methanol (Sigma Chemical Co., St. Louis, MO; spectroscopic grade) solution were recorded with a Mark V Jobin-Yvon dichrograph. Several scans between 185 and 260 nm were averaged and the different conformational contents were estimated from published standard ellipticity values (14).

In macroscopic conductance experiments, lipid bilayers were formed over a 125 μm hole in a 25 μm thick PTFE film by apposition of two monolayers (15). These membranes were submitted to triangular voltage ramps (40 s per cycle). For resolution of fast single-channel fluctuations, temperature had to be lowered to 7°C and lipid bilayers were formed at the tip of patch-clamp pipettes (16). In both configurations, the electrolytic solution was 1 M KCl, both sides, and the same lipid (from Avanti Polar Lipids, Alabaster, AL) mixture was used: 1-palmitoyl-2-oleoyl-phosphatidylcholine (POPC)/dioleoylphosphatidylethanolamine (DOPE), 7/3, 1% and 0.1% in hexane for macroscopic and single-channel conductances experiments, respectively. Before adding the peptide from a methanolic stock solution to the cis- (or positive side), the bare membrane was checked, under an applied potential, for stability and absence of channel-like events. As a further control, in the case of diBLP14A, an eluate sample of volume corresponding to the normal test and taken directly out of the HPLC column, just before the repurified peak (Fig. 1 *C*), did not induce any conductance. Single-channel fluctuations, filtered at 3 kHz and stored on a digital tape recorder (DTR 1200; Biologic, Claix, France) at a rate of 2.10^4 points/s, were subsequently analyzed through Satori v. 3.01 software from Intracel Ltd. (Cambridge, UK).

TABLE 1 FAB-derived and theoretical molecular masses

Peptide	Experimental	Expected
diBL	2187.4	2187.4
diBLP2A	2160.9	2161.3
diBLP14A	2161.4	2161.3

TABLE 2 Apparent mean number of peptide molecules forming the channels as derived from the macroscopic current-voltage curves of Fig. 4

Peptide	V_a Concentration dependence	V_c Voltage dependence	n Apparent mean number of monomers	% α-helical content
	mV	*mV*		
diBL*	54	6.7	8	70
diBLP2A	75	8.2	9	80
diBLP14A	42	7.2	6	63

* See reference 17.
The last column recalled circular dichroism data.

RESULTS

As shown by the circular dichroism spectra of Fig. 3, substitutions of proline by alanine residues in either positions 2 or 14 do not profoundly alter the secondary structure of the analogues in methanolic solution as compared with the parent molecule. Nevertheless, as estimated at 208 nm, where the contributions of minor conformations are minima, the α-helical content shifts from 70% for diBL to 80% for diBLP2A. By contrast, if the substitution occurs at position 14 (diBLP14A), the helicity is slightly reduced (to 63%). These values apply too for the 191 nm peak.

When large bilayers are doped with sufficient aqueous concentrations of either peptide and submitted to a triangular voltage ramp, a macroscopic current develops in the positive gradient (the peptide being added to the cis-side). As expected, the Pro_2-Ala_2 substitution in peptide diBLP2A does not impede the high voltage-dependence characteristic of alamethicin channels and also of diBL (17), since a steep exponential branch is still observed above a voltage threshold (Fig. 4 *A*). To our surprise, this same pattern is retained when peptide diBLP14A is tested.

However, significant differences appear when the concentration dependence is studied. For each peptide, the aqueous concentration is doubled and, after ensuring that equilibrium is reached, the shift in the voltages V_c at which the exponential branches cross a reference conductance is noted. The concentration dependence of diBLP2A macroscopic conductance is comparable to those displayed by diBL and alamethicin (17). The Pro_{14}-Ala_{14} substitution alters this concentration dependence: the diBLP14A concentration required to reach

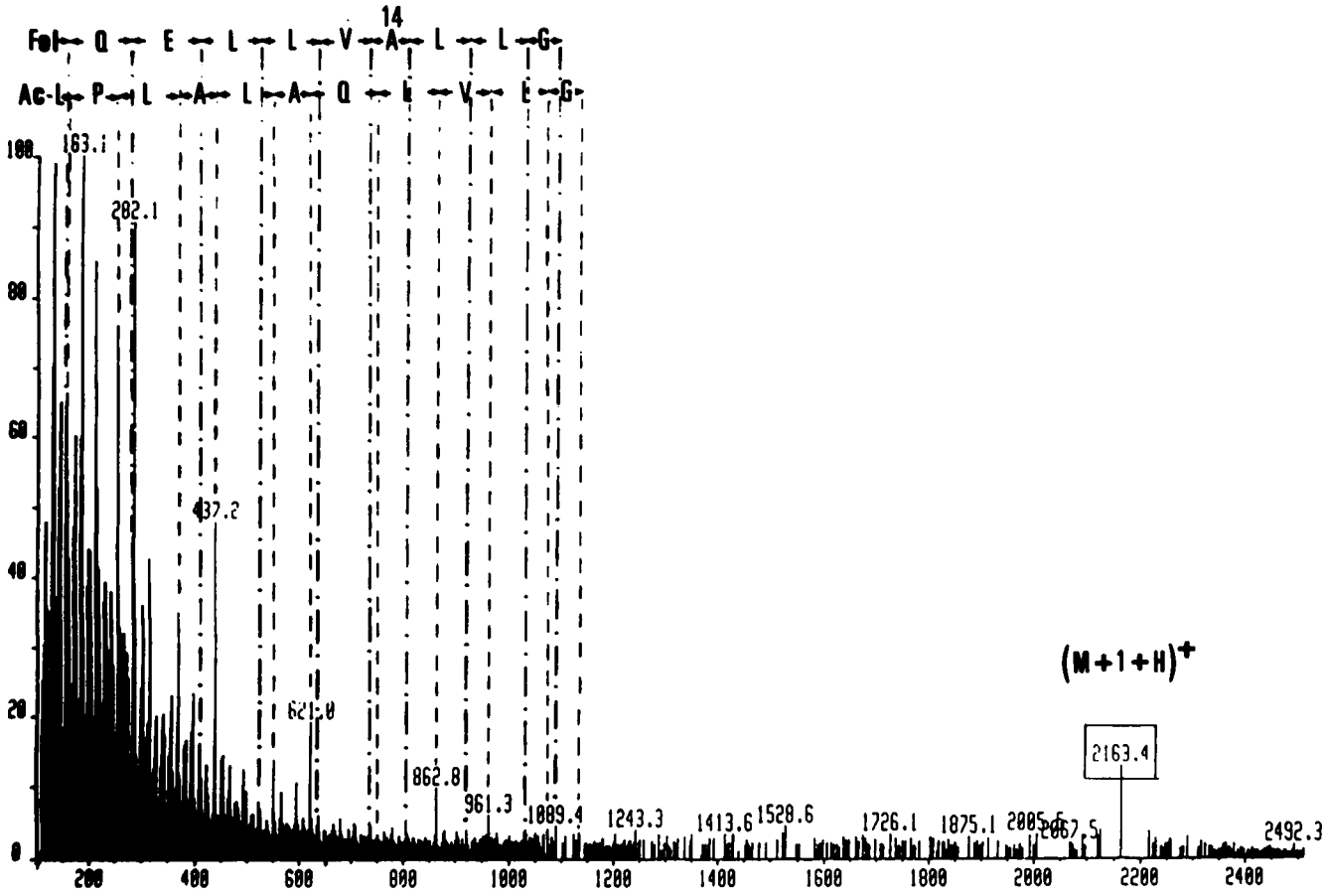

FIGURE 2 Positive ion FAB mass spectrum for peptide diBLP14A, dissolved in α-thioglycerol. Ions acceleration: 8 KeV. Fragmentation spectrum (relative intensities as a function of mass) starting either from C-terminus (*upper row*) or N-terminus (*lower row*). The framed figure gives the molecular peak.

the reference conductance is four to five times higher than with diBLP2A (Fig. 4 *B*). Note also the development of a voltage-independent conductance at these high concentrations and more symmetrical current-voltage curves.

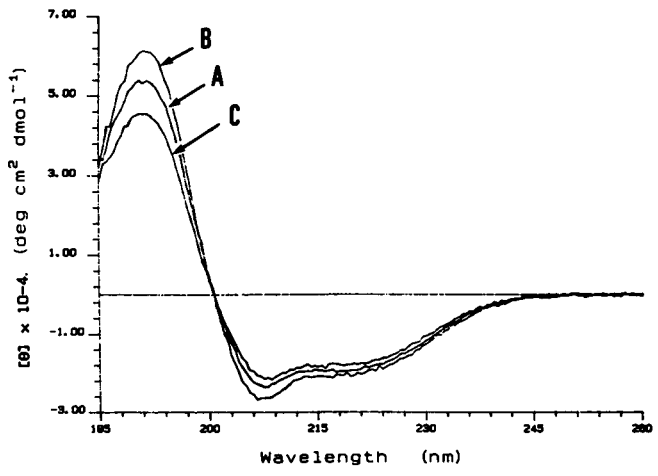

FIGURE 3 Circular dichroism spectra of the three analogues in methanol (1 mg/ml). Pathlength: 0.01 cm, 10 averaged scans and room temperature. (Spectrum *A*) peptide diBL; (*B*) diBLP2A; (*C*) diBLP14A.

The apparent mean number n of molecules in the conducting aggregates can be estimated through an analysis already described for alamethicin (4). V_a is defined as the V_c shift for an e-fold change in peptide concentration, and V_e is the voltage increment producing an e-fold conductance change. n is then, simply, V_a/V_e. Table 2 shows that whereas diBLP2A would form hardly larger channels than the parent molecule, the number of monomers composing diBLP14A channels is markedly reduced.

In Fig. 5 are compared examples of single-channel current recordings displayed by the three peptides in the same voltage range. As a general rule, both Pro-Ala substitutions lead to faster current fluctuations, the effect being the strongest with diBLP14A. Nevertheless, even with this latter analogue (repurified, see Fig. 1 *C*) for which current fluctuations are not so well resolved, multistates are still observed although their number is reduced in agreement with macroscopic conductance analysis (Table 2).

The main single-channel conductance parameters of the three peptides are listed in Table 3. The Pro_2-Ala_2

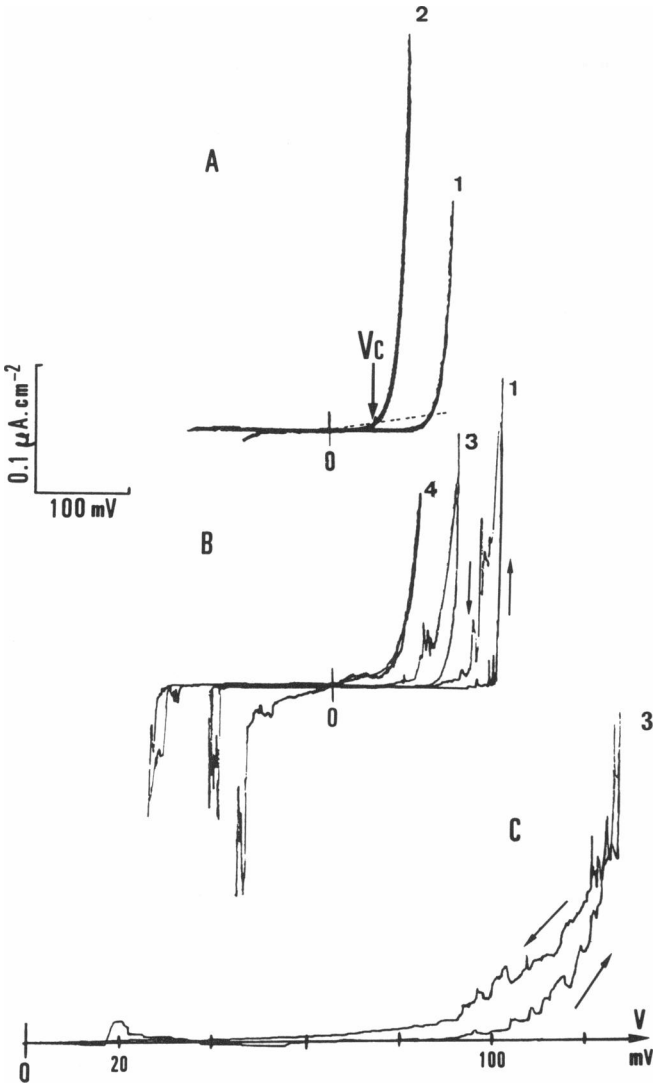

FIGURE 4 Macroscopic current-voltage curves compared for diBLP2A (*A*) and diBLP14A (*B*) at increasing peptide aqueous concentrations: 5 10^{-8} M (curve 1), 10^{-7} M (curve 2), 2 10^{-7} M (curve 3), and 4 10^{-7} M (curve 4). The dashed line in *A* represents a reference conductance (100 nS · cm^{-2}) defining characteristic voltages (V_c). 1 M KCl both sides and room temperature. Part *C* is an enlargement of curve 3 from part *B*.

substitution does not significantly affect either single-channel conductance of the substates or their probability of being open. The main effect is the shortening of the open lifetimes, much more conspicuous in the case of diBLP14A. This is further illustrated with histograms on the right-hand side of Fig. 5.

DISCUSSION

The replacement of Pro_2 by Alanine leaves a free hydrogen which cannot be engaged in a 5-1 intra-helical bond. On the other hand, the substitution of Pro_{14} by Ala should restore a 5-1 bond between Leu_{10}-carbonyl and Ala_{14} amido group. The expectations of a slightly reduced ellipticity for diBLP2A and a greater α-helical content for diBLP14A are not confirmed by the present circular dichroism data. Caution is required here since these changes amount to only ~10% and no systematic study has yet been undertaken to assess the influence of proline residues at different positions in molecules used for ellipticity standards.

It is interesting to note that, even if these changes in α-helical content are hardly significant, they roughly correlate (see Table 2) with the equally slight changes in the number of molecules per aggregate: an increased ellipticity would favor bigger aggregates. The same correlation with voltage-dependence modulation does not seem so straightforward. There is, however, some indication for a surprising inverse correlation (higher helical content tentatively associated with lower voltage dependence) which deserves further investigation and would argue for an optimal initial content in β-sheet and its eventual transconformation into α-helix, driven by the large electric field, as an important step in the gating (4).

In agreement with a recent study of melittin P14A (18), the Pro_{14}-Ala_{14} substitution in our synthetic alamethicin analogue alters the concentration dependence of macroscopic conductance but we do not find evidence for a lesser voltage dependence. Since the replacement of Pro by Ala may align both moieties of the molecule, the packing of the monomers in the aggregate would then be seriously perturbed to accommodate the bulky C-terminals. Note that both macroscopic (*n*, number of monomers, Table 2) and single-channel conductance analyses (open substates probability) agree for smaller conducting aggregates for diBLP14A. Presumably, Pro_{14}, allowing the C-termini to project laterally away from the main helical axis, favors the building up of larger conducting aggregates (4, 19). A tighter packing of the helices all the way through the intramembrane aggregate, instead of the usual funnel shape of the alamethicin channels, would plausibly increase energy barriers for ion crossing and explain the observed lower single-channel conductances. Likewise, α-helical coiled coils of monomers would shorten the aggregates, reduce the matching with the bilayer thickness, and result in faster channels.

As expected, the Pro_2-Ala_2 substitution induced little effects regarding either voltage-dependence or single-channel substates conductances. Since Ala presents a higher hydrophobicity index, the reduced open lifetimes could reflect a less efficient transient anchoring of the N-terminus at the trans-interface or an increased tilting of the helices relative to the membrane plane (20).

Although prolines, especially in position 14, are definitely most helpful for the development of well resolved multistate conductances, these results, arguing they are not compulsory for alamethicin-like events, raise some difficulties in a straightforward interpretation of the "barrel-stave" model (3). Former versions emphasizing dipolar interactions with the electric field (4) and "flip-flop" gating (21) might still be accurate. Finally, while

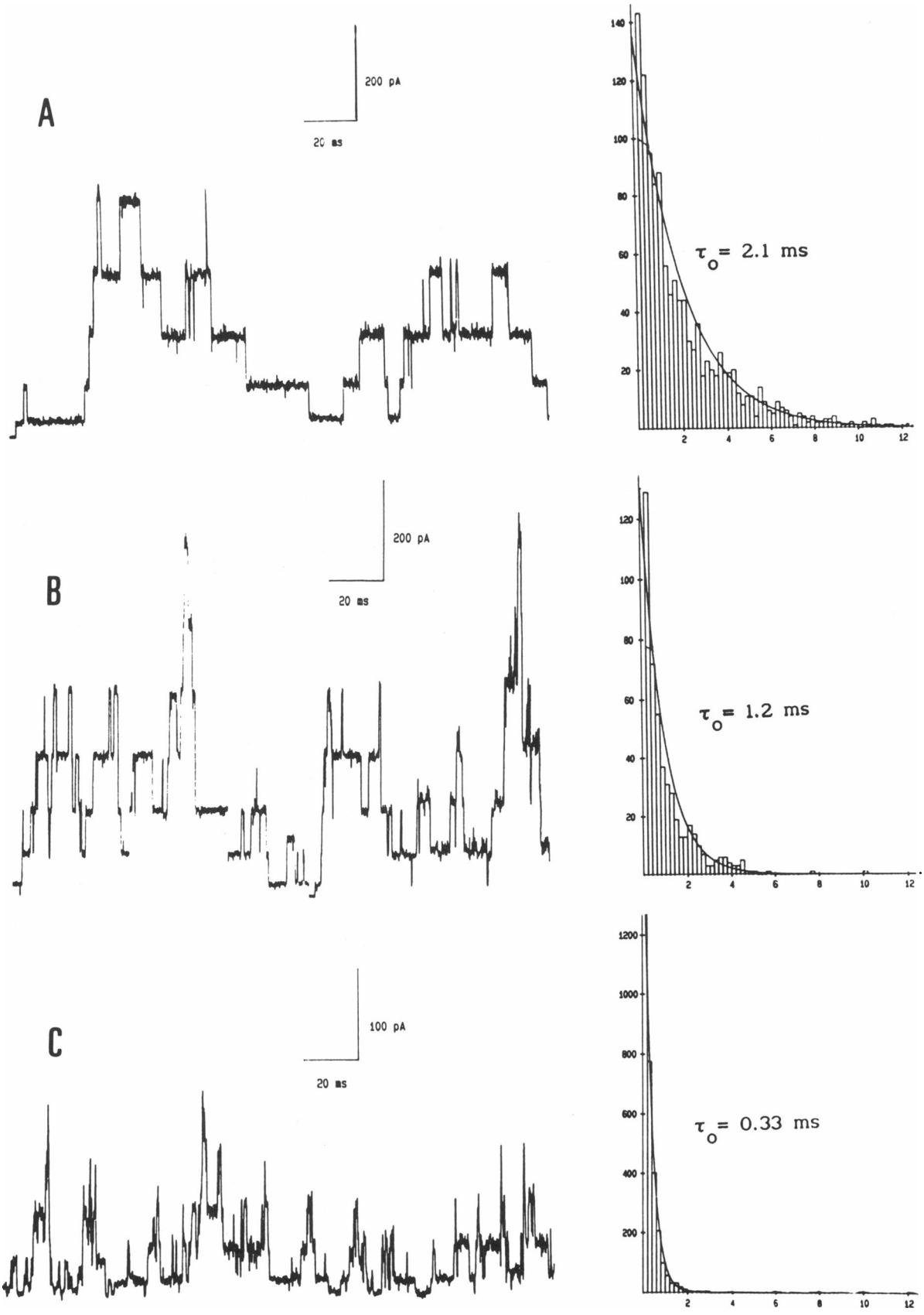

FIGURE 5 Single-channel current fluctuations induced by the three analogues at 7°C; 1 M KCl both sides and same lipid as above (POPC/DOPE: 7/3). Peptide concentrations: 2 10^{-9} M throughout and applied voltages, 150 mV for diBL (trace *A*); 135 mV for diBLP2A (trace *B*); and 155 mV for diBLP14A (trace *C*). On the right are shown the associated histograms of single-channel open lifetimes for the same substate (number 3).

TABLE 3 **Single-channel parameters compared for the three analogues**

	Substate	γ	P	τ_o
		pS		*ms*
Peptide diBL	1	220	0.38	3.0
	2	700	0.36	2.9
	3	1,350	0.18	2.1
	4	2,230	0.07	1.3
	5	3,260	0.01	0.7
Peptide diBLP2A	1	190	0.35	1.6
	2	710	0.35	1.7
	3	1,420	0.18	1.2
	4	2,310	0.09	1.1
	5	3,320	0.03	0.8
Peptide diBLP14A	1	70	0.47	0.28
	2	260	0.37	0.37
	3	550	0.14	0.33
	4	1,100	0.02	0.30

For each substate: γ = single-channel conductance, P = probability for a substate of being open (within bursts, rest, or closed state excluded), and τ_o = mean open lifetime (events shorter than 5% of the mean are excluded from the analysis).

this study does not yet prove that bending does not occur in the substituted analogues, it suggests (in opposition to a recent work [22]) that helix bending might well not be so critical for the gating of voltage-dependent ion channels.

This work was supported by GDR G 0964 from CNRS: "Canaux peptidiques transmembranaires."

Received for publication 1 May 1991 and in final form 9 April 1992.

REFERENCES

1. Lear, J. D., Z. R. Wasserman, and W. F. DeGrado. 1988. Synthetic amphiphilic peptide models for protein ion channels. *Science (Wash. DC).* 240:1177–1181.
2. Boheim, G. 1974. Statistical analysis of alamethicin channels in black lipid membranes. *J. Membr. Biol.* 19:277–303.
3. Fox, R. O., and F. M. Richards. 1982. A voltage-gated ion channel model inferred from the crystal structure of alamethicin at 1.5 Å resolution. *Nature (Lond.).* 300:325–330.
4. Hall, J. E., I. Vodyanoy, T. M. Balasubramanian, and G. R. Marshall. 1984. Alamethicin: a rich model for channel behavior. *Biophys. J.* 45:233–247.
5. Cascio, M., and B. A. Wallace. 1988. Conformation of alamethicin in phospholipid vesicles: implications for insertion models. *Proteins: structure, function and genetics.* 4:89–98.
6. Molle, G., H. Duclohier, S. Julien, and G. Spach. 1991. Synthetic analogues of alamethicin: effect of C-terminal residue substitution and chain length on the ion channel lifetimes. *Biochim. Biophys. Acta.* 1064:365–369.
7. Jung, G., R. P. Hummel, K. P. Voges, C. Toniolo, and G. Boheim. 1987. Voltage-dependent helical channel formers: structure and function. *In* Protides of the Biological Fluids. Vol. 35. Pergamon Press, Oxford-New York. 485–488.
8. Duclohier, H., G. Molle, and G. Spach. 1989. Ion channels made from bundles of alpha-helices: the influence of the intramembrane helical length. *In* Peptides, 1988, Proceedings of the 20th European Peptide Symposium. G. Jung and E. Bayer, editors. Walter de Gruyter, Berlin. 357–359.
9. El Hajji, M., S. Rebuffat, D. Lecommandeur, and B. Bodo. 1987. Isolation and sequence determination of trichorzianines A, antifungal peptides from Trichoderma harzianium. *Int. J. Peptide Protein Res.* 29:207–215.
10. Merrifield, R. B. 1963. Solid phase peptide synthesis. I. The synthesis of a tetrapeptide. *J. Am. Chem. Soc.* 89:2149–2154.
11. Molle, G., J.-Y. Dugast, H. Duclohier, P. Daumas, F. Heitz, and G. Spach. 1988. Ionophore properties of a synthetic alpha-helical transmembrane fragment of the mitochondrial H^+ ATP synthetase of Saccharomyces cerevisiae. *Biophys. J.* 53:193–203.
12. Molle, G., and J.-Y. Dugast. 1990. Synthèse sur support solide de peptides comportant un residu aminoalcool C-terminal. *Tetrahedron Lett.* 31:6355–6356.
13. Lee, T. D. 1986. Fast atom bombardment and secondary ion mass spectrometry of peptides and proteins. *In* Methods of Protein Microcharacterization. J. E. Shively, editor. The Humana Press, Clifton, NJ. 403–441.
14. Blout, E. R. 1973. Polypeptides and proteins. *In* Fundamental Aspects and Recent Developments in Optical Rotatory Dispersion and Circular Dichroism. F. Ciardelli and P. Salvadori, editors. Heyden and Sons Ltd., London. 352–372.
15. Montal, M., and P. Mueller. 1972. Formation of bimolecular membranes from monolayers and study of their properties. *Proc. Natl. Acad. Sci. USA.* 69:3561–3566.
16. Hanke, W., C. Methfessel, W. Wilmsen, and G. Boheim. 1984. Ion channel reconstitution into lipid bilayer membranes on glass patch pipettes. *Bioelectrochem. Bioenerg.* 12:329–339.
17. Molle, G., J.-Y. Dugast, H. Duclohier, and G. Spach. 1988. Conductance properties of des-Aib-Leu-des-Pheol-Phe-alamethicin in planar lipid bilayers. *Biochim. Biophys. Acta.* 938:310–314.
18. Dempsey, C. E., R. Bazzo, T. S. Harvey, I. Syperek, G. Boheim, and I. D. Campbell. 1991. Contribution of proline-14 to the structure and actions of melittin. *FEBS Lett.* 281:240–244.
19. Boheim, G., S. Gelfert, G. Jung, and G. Menestrina. 1987. α-helical ion channels reconstituted into planar bilayers. *In* Ion Transport through Membranes. K. Yagi and B. Pullman, editors. Academic Press, Tokyo. 131–145.
20. Wu, Y., and H. W. Huang. 1991. Alamethicin-membrane interactions and voltage-gating mechanism of alamethicin channel. *Biophys. J.* 59:625 *a.* (Abstr.)
21. Boheim, G., W. Hanke, and G. Jung. 1983. Alamethicin pore formation: voltage-dependent flip-flop of α-helix dipoles. *Biophys. Struct. Mech.* 9:181–191.
22. Woolfson, D. N., R. J. Mortishire-Smith, and D. H. Williams. 1991. Conserved positioning of proline residues in membrane-spanning helices of ion-channel proteins. *Biochem. Biophys. Res. Commun.* 175:733–737.